



HAL
open science

Theoretical insights into the formation and stability of radical oxygen species in cryptochrome

Padmabati Mondal, Miquel Huix-Rotllant

► **To cite this version:**

Padmabati Mondal, Miquel Huix-Rotllant. Theoretical insights into the formation and stability of radical oxygen species in cryptochrome. *Physical Chemistry Chemical Physics*, 2019, 21, pp.8874-8882. 10.1039/C9CP00782B . hal-02088383

HAL Id: hal-02088383

<https://amu.hal.science/hal-02088383>

Submitted on 2 Apr 2019

HAL is a multi-disciplinary open access archive for the deposit and dissemination of scientific research documents, whether they are published or not. The documents may come from teaching and research institutions in France or abroad, or from public or private research centers.

L'archive ouverte pluridisciplinaire **HAL**, est destinée au dépôt et à la diffusion de documents scientifiques de niveau recherche, publiés ou non, émanant des établissements d'enseignement et de recherche français ou étrangers, des laboratoires publics ou privés.

Cite this: DOI: 10.1039/xxxxxxxxxx

Theoretical insights into the formation and stability of radical oxygen species in cryptochrome

Padmabati Mondal,^{*a} and Miquel Huix-Rotllant^{*a}

Received Date
Accepted Date

DOI: 10.1039/xxxxxxxxxx

www.rsc.org/journalname

Abstract

Cryptochrome is a blue-light absorbing flavoprotein containing a flavin adenine dinucleotide (FAD) cofactor. FAD can accept up to two electrons and two protons, which can be subsequently transferred to substrates present in the binding pocket. It is well known that reactive oxygen species are generated when triplet molecular oxygen is present in the cavity. Here, we investigate the formation and stability of radical oxygen species in *Drosophila melanogaster* cryptochrome using molecular dynamics simulations and electronic structure calculations. We find that superoxide and hydroxyl radicals in doublet spin states are stabilized in the pocket due to attractive electrostatic interactions and hydrogen bonding with partially reduced FAD. These findings validate from a molecular dynamics perspective that $[\text{FAD}^{\bullet-} - \text{HO}_2^{\bullet}]$ or $[\text{FADH}^{\bullet} - \text{O}_2^{\bullet-}]$ can be alternative radical pairs at the origin of magnetoreception.

1 Introduction

Cryptochromes are a type of flavoproteins that absorb blue-UV/A light.¹ They are found throughout the biological kingdom (microbes, plants, animals, etc.)^{2,3}, involved in several biological processes like plant growth or entrainment of the circadian clock in animals.^{1,4-7} Cryptochromes contain vitamin B₂ acting as photoactive oxidizing agent, found either in the form of flavin mononucleotide (FMN) or flavin adenine dinucleotide (FAD). The vitamin B₂ cofactor, also known as riboflavin, is common to all flavoproteins, and it is responsible for their functionality. It consists of a lumiflavin moiety acting as chromophore and a pentane-2,3,4-triol side chain. Lumiflavin is a good oxidizing agent and a strong base, accepting up to two electrons and two protons. The oxidizing potential is increased upon light absorption.

Initially, the cofactor is usually found in its fully oxidized form. The oxidized FAD (FAD_{ox}) can then be reduced to the anionic radical semi-quinone form ($\text{FAD}^{\bullet-}$) via electron transfer from a residue near the flavin chromophore. In cryptochromes, the most widely accepted mechanism is that this electron is transferred from a nearby tryptophan that is concomitantly oxidized to $\text{TrpH}^{\bullet+}$.⁸ The anionic radical $\text{FAD}^{\bullet-}$ is a strong base that can accept a proton to generate the neutral semi-quinone FADH^{\bullet} . The origin of this proton depends on the type of cryptochrome. For *Arabidopsis thaliana* cryptochrome, an aspartic acid donates a proton to FAD and $\text{TrpH}^{\bullet+}$ subsequently transfer another proton

to the aspartate, ending up in a neutral tryptophanyl radical Trp^{\bullet} and a neutral semi-quinone FADH^{\bullet} .⁸ For *Drosophila melanogaster* cryptochrome, the participating residues in this proton transfer process have not yet been clearly identified. The FADH^{\bullet} can still act as a photooxidizer and a photobase, absorbing in the visible region, leading to the anionic reduced form FADH^- when accepting one electron and the neutral reduced form FADH_2 when sequentially accepting a proton.⁹⁻¹¹

Cryptochromes have been proposed as plausible candidates for explaining the light-dependent magnetic field sensors, a capacity of certain animals to guide by perceiving the geomagnetic field (so-called magnetoreception).⁹⁻¹¹ Spin-correlated radical pairs between flavin and tryptophan ($\text{FADH}^{\bullet} - \text{Trp}^{\bullet}$) generated by photoreduction in plant cryptochrome have been reported to be at the origin of magnetoreception.^{8-10,12} This is known as the radical pair mechanism of magnetoreception (hereafter referred as “conventional” radical pair). A recent study showed that tryptophan triad might not be necessary for magnetoreception in *Drosophila melanogaster*,¹³ opening up the route for alternative radical pairs in certain cryptochromes. It has been proposed FADH^{\bullet} can form a radical pair with oxygen superoxide ($\text{O}_2^{\bullet-}$) in lieu of tryptophan.^{14,15} Recent theoretical studies indicate that the $\text{FADH}^{\bullet} - \text{O}_2^{\bullet-}$ radical pair could resist better to decoherence phenomena, thus being a better candidate for magnetoreception than the tryptophan-flavin pair.^{16,17}

Superoxide can be formed in cryptochromes during the re-oxidation reaction of the fully reduced anionic form of FAD in the dark environment ($\text{FADH}^- \rightarrow \text{FADH}^{\bullet} \rightarrow \text{FAD}_{\text{ox}}$). There are experimental evidences that reactive oxygen species (ROS) can

^aAix-Marseille Univ, CNRS, ICR, Marseille, France. E-mail: padmabati.mondal@gmail.com; miquel.huixrotllant@univ-amu.fr

† Electronic Supplementary Information (ESI) available: [details of any supplementary information available should be included here]. See DOI: 10.1039/b000000x/

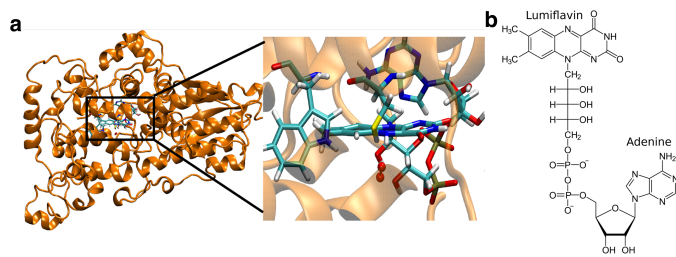


Fig. 1 (a) Structure of dmCry–O₂ system. The zoomed active site of dmCry with FAD_{ox}–O₂ is shown as an inset in the right hand side (b) Structure of flavin adenine dinucleotide.

be present in the active site of cryptochrome.^{18–21} Combined molecular dynamics simulation and kinetic studies confirm that indeed oxygen molecule can access the flavoprotein binding site via multiple pathways facilitating catalytic oxidation procedure.²² While several studies focused on the photo-reduction reaction,^{8,11,12,23–25} not much attention has been given to the study of the re-oxidation reaction.^{18,26}

Here, we perform a thorough molecular dynamics study of different oxygen species including the ROS within the *Drosophila melanogaster* cryptochrome depending on the redox and protonation states of flavin chromophore. In order to explain the oxidation state of oxygen complexed with different redox forms of FAD, multi-configurations electronic structure calculations were performed. We find that the ROS stay close to the flavin chromophore via strong attractive electrostatic interactions or hydrogen bonding, while the triplet molecular oxygen diffuses out of the flavin pocket when FAD is reduced. These results support the existence of [FAD^{•–}–HO₂[•]] or [FADH[•]–O₂^{•–}] as alternative radical pair involving superoxide as the basis for the magnetoreception in *Drosophila melanogaster* cryptochrome.

2 Computational Details

The initial protein structure (with FAD co-factor, see Figure 1) is taken from the chain B of the crystal structure of *Drosophila melanogaster* cryptochrome (dmCry), PDBID:4K03. In order to obtain the initial structure of dmCry–O₂ complex, an oxygen molecule has been placed in the active site according to the gas-phase optimized structure of FAD–O₂ complex obtained at the wB97x-D/6-31G* level.^{27,28} Molecular dynamics simulations based on several random initial conditions of the FAD–O₂ complex have been performed to determine the stability of the results (see Supporting Information). The initial dmCry–O₂ structure with FAD_{ox}–O₂ (A) is neutralized with 13 Na⁺ ions and solvated in a 105 × 105 × 105 Å³ water box rendering the total system size of 114,012 atoms. The other protonation states of the dmCry–O₂ complex have been generated from the initial dmCry–O₂ structure of the fully oxidized form. All molecular dynamics (MD) simulations were performed using Gromacs software.²⁹ The solvated and ionated dmCry–O₂ structures were then minimized and equilibrated using NVT (for 200 ps) and NPT (1 ns) ensembles at T=300 K. A production run of 10 ns was performed for each system. The electrostatic interactions between FAD and oxygen are

represented by the set of charges calculated considering oxygen as superoxide, hydroperoxyl radical or triplet as well as corresponding redox and spin state of FAD.

Charmm27 force fields^{30,31} have been employed for the protein scaffold. The bonded, angular, dihedral and van der Waals parameters of FAD species are taken from CGENFF database and are considered to be the same for all possible redox and protonated states.³² The bonded parameters for oxygen species are taken from density functional theory employing the range-separated exchange-correlation functional with dispersion correction (wB97x-D) and 6-31G* atomic basis set. These quantum chemical calculations have been performed using GAUSSIAN16.³³ The electrostatic part of the force fields for the FAD and O₂ species has been reparameterized based on Mulliken atomic charges obtained from density functional theory employing wB97x-D functional and 6-31G* atomic basis set.^{27,28} Since Charmm force field relies on Mulliken atomic charges as the initial guess for the protein electrostatic interactions,^{34,35} we have employed them for the FAD and oxygen species to be consistent. To assess the validity of the force field, we have compared molecular dynamics simulations using our Mulliken atomic charges and Merz-Kollman electrostatic potential fitting atomic charges, leading to similar evolution for the C_{4a}–OO1 distance, indicating a similar description of the electrostatic interactions between oxygen and FAD (see Supporting Information). Mulliken charges for the optimized structure for the different redox states of FAD, triplet oxygen ³O₂ and doublet superoxide ²O₂^{•–} and hydroxyl ²HO₂[•], according to their total charge and spin multiplicity have been used as the electrostatic force fields parameters for the MD simulations. Hereafter, the superscripts on the left indicate the spin multiplicity of the fragment.

The electronic structure calculations for the radical and anionic FAD–O₂ systems were performed using state-averaged Complete Active Space Self Consistent Fields (SA-CASSCF) method with second-order perturbation theory correction (CASPT2). The state-averaged for five electronic states using an active space of (11,12) for radicals and (12,12) for the rest. For multi-configuration calculations, the ANO-RCC-VDZP basis set has been employed.³⁶ For these calculations, OpenMolcas package has been used.³⁷

3 Results and discussion

In Figure 2a, we summarize the redox forms of FAD starting from the blue-light absorption of FAD_{ox}, supposing that the electron is donated by a residue near the cavity.^{9,10} When triplet oxygen is present inside the cavity, the FAD–O₂ complex can exist in several spin states (see Figure 2b). Initially, the complex is in a total triplet state ³[FAD_{ox}–O₂] composed of singlet ¹FAD_{ox} (fully oxidized FAD) and triplet molecular oxygen ³O₂. Upon reduction of FAD by tryptophan, the complex can exist either in total doublet ²[FAD^{•–}–O₂] or quartet state ⁴[FAD^{•–}–O₂], depending on the relative orientation of oxygen spin with respect to the FAD electron. Subsequently, a proton can be transferred to neutralize this charge generating again a doublet ²[FADH[•]–O₂] or a quartet ⁴[FADH[•]–O₂] with the partially reduced neutral semi-quinone ²FADH[•]. When a second electron is transferred, the complex can

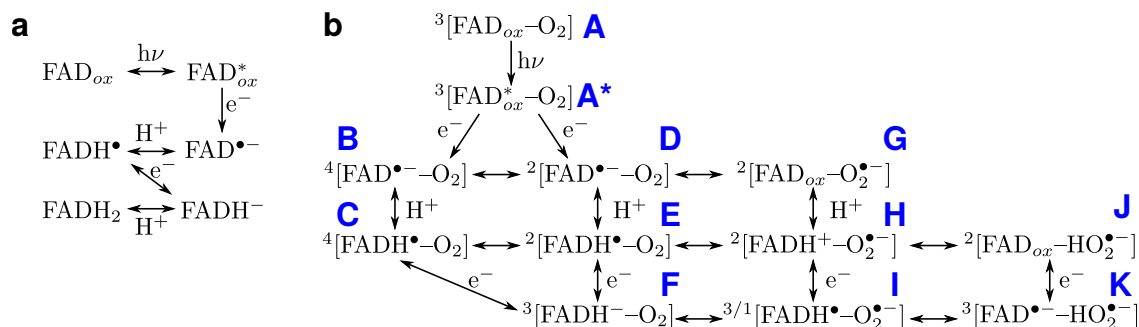


Fig. 2 (a) Redox and acid-base reactions path of flavin adenine dinucleotide. The reduction can be induced photochemically by absorption of blue light by FAD. (b) Redox and electron exchange reactions path involving FAD and oxygen. For convenience, each system is labelled with a one letter tag (A-K) in blue.

be in singlet ${}^1[\text{FADH}^--\text{O}_2]$ or triplet ${}^3[\text{FADH}^--\text{O}_2]$. Here, we have only considered FAD as the electron/proton acceptor and oxygen as a spectator. However, oxygen can re-oxidize reduced FAD (FADH^{\bullet} or FADH^-) and accept protons. This would imply an intramolecular reaction that leaves the total charge and spin of the complex unchanged. The resulting structures produce the ROS, ${}^2\text{O}_2^{\bullet-}$ or hydroxyl ${}^2\text{HO}_2^{\bullet}$ radicals.

The main reaction paths involving FAD and O_2 are summarized in Figure 2b. The initial state of cryptochrome is ${}^3[\text{FAD}_{ox}-\text{O}_2]$ (A). When photoexcited (A^*), it can be reduced by a nearby tryptophan. When the semireduced FAD- O_2 complex is in quartet (B), molecular oxygen is a spectator, and the next proton ($\text{B} \rightarrow \text{C}$) and the subsequent electron transfer ($\text{C} \rightarrow \text{F}$) can only be accepted by FAD. Instead, when reduced anionic FAD is forming a doublet with O_2 (D), the next proton and electron can be accepted by $\text{FAD}^{\bullet-}$ ($\text{D} \rightarrow \text{E} \rightarrow \text{F}$). There is though the possibility that superoxide is formed (G) and thus an equivalent superoxide channel exists ($\text{G} \rightarrow \text{H} \rightarrow \text{I}$). Finally, when a proton is transferred to oxygen, two hydroxyl radicals can be formed with oxidized FAD (J) and partially reduced FAD (K). The systems D and E (total doublet with triplet oxygen and radical FAD) produce the same partial charges as B and C, respectively. They are only distinguished by the orientation of the triplet spin, either parallel to the radical spin on FAD (quartet) or anti-parallel (doublet). Therefore we performed the simulations for the simpler quartet system B and C, assuming them equivalent to the system D and E, respectively, in the molecular dynamics simulation.

3.1 Presence of oxygen species in the binding pocket

A fundamental issue to investigate the role of O_2 in cryptochromes is to know which of these species are stabilized in the active site, near the flavin moiety. For this purpose, we have investigated several flavin-oxygen complexes for different spin and protonation states. For this study, we have defined the active site as the cavity around FAD by a sphere with radius of 5 Å.²² Along the trajectories, we collect the distances between the OO1 atom of the oxygen and the C4a atom (the FAD atom known to interact with oxygen species)²⁶ during the 10 ns MD simulations.

The time-evolution of distances is shown in Figure 3. The C4a-OO1 distance for the systems with triplet oxygen (Figure 3a)

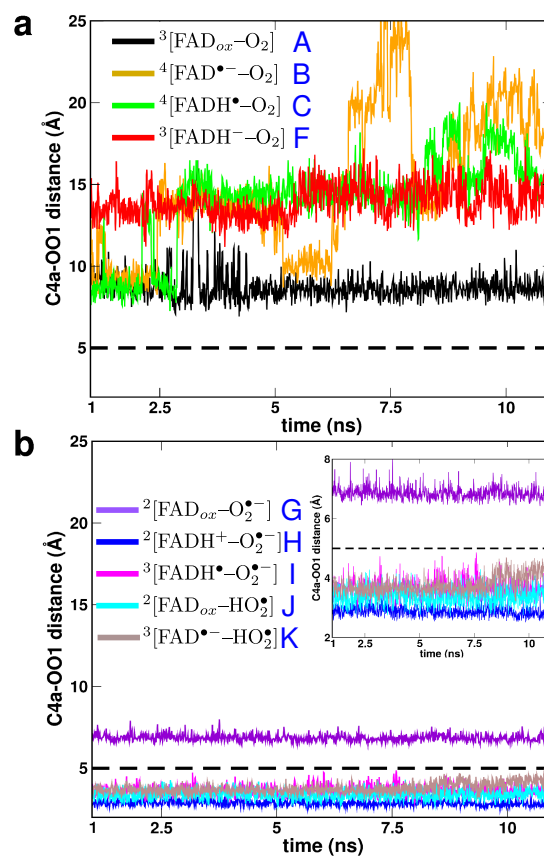


Fig. 3 The distance between C4a atom of the chromophore and OO1 atom of the oxygen species for 10 ns of MD simulation of each system. The horizontal dashed black line refers to the radius of the C4a cavity. The distances for the dynamics of neutral and radical oxygen species are separated in the upper (a) and lower panel (b), respectively. The inset of panel b shows the C4a-OO1 distances for radical oxygen species in a optimized y-scale.

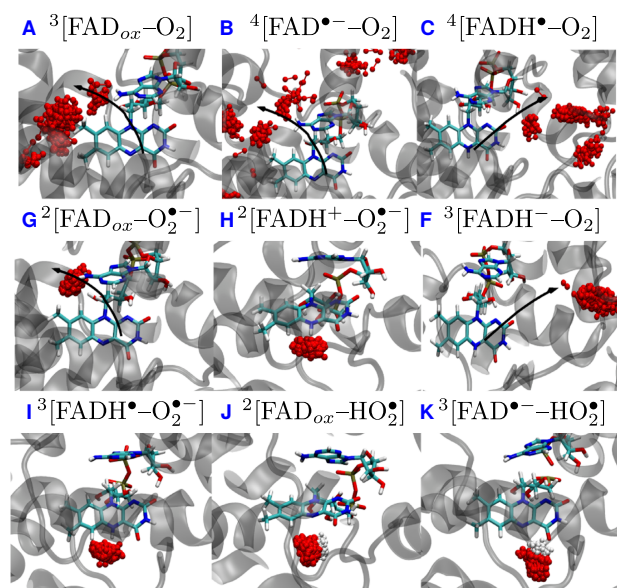


Fig. 4 Specific position of the oxygen species (in red CPK representation) in dmCry–O₂ for all systems (A to K) as clusters from 200 snapshots taken at 50 ps intervals during 10 ns of simulation. The black arrows indicate the diffusing pathway of oxygen species.

show in general a rather repulsive interaction with FAD. The distance between oxygen and FAD depends strongly on the redox state of FAD. In the initial FAD_{ox} form, molecular oxygen is stabilized around 3 Å away from the binding pocket. This is a steady value with small fluctuations on the average distance, in accordance with the fact that oxygen is present inside the protein.^{22,26} For the radical forms (FAD^{•-} and FADH[•]), oxygen diffuses away from the binding pocket. Large fluctuations are observed for these C4a-OO1 distances, indicating a strong repulsive interaction between reduced FAD and ³O₂, the distance of which can be as large as 20 Å. Finally, for the anionic reduced form (FADH⁻), oxygen is stabilized on an average at around 9 Å far from the pocket boundary. This suggests a slow reoxidation reaction for FADH⁻ → FADH[•] and an even slower FADH[•] → FAD_{ox}, in accordance with kinetic experiment.¹⁸ Upon electron transfer from reduced flavin to oxygen, flavin is reoxidized and superoxide is formed. Subsequently, FAD can be again reduced absorbing a second photon thus forming several radical pairs with either superoxide or hydroxyl radicals. In Figure 3b, we observe that these radical oxygen species are all stabilized inside the binding pocket, very close to FAD. On average, these distances are around 3-4 Å and undergo very low fluctuation. This indicates a strong attractive electrostatic interaction of oxygen superoxide and hydroxyl radicals with the residues in the binding pocket. This would suggest that absorbing one photon is required to generate superoxide and another photon can generate a radical pair and stabilizes superoxide inside the pocket.

In order to clarify the interaction between the oxygen species and the cavity, we analyze the specific binding location or specific diffusion pathway of the oxygen species. For this purpose, we performed a cluster plot of oxygen species from 200 snapshots

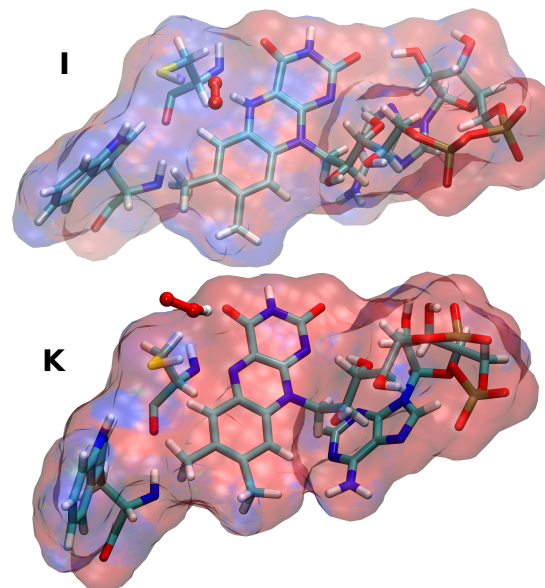


Fig. 5 The electrostatic potential of FADH[•], Trp420 and Cys416 felt by the superoxide and hydroperoxyl radical for ³[FADH[•]–O₂^{•-}] (I) and ³[FAD^{•-}–HO₂] (K) system. The electrostatic potential (ESP) is calculated using Adaptive Poisson-Boltzmann Solver (APBS)³⁸ in gas phase. The ESP is shown in a RGB (Red-Green-Blue) color scale in a range of -0.05 to 0.05 k_bT/e .

taken at 50 ps intervals during 10 ns trajectories of dmCry–O₂ complex. The results are shown in Figure 4. One can observe that the position of the oxygen species is different depending on whether it is a ³O₂ or ²O₂^{•-} or a HO₂[•]. When oxygen is in superoxide form, it stays near the flavin stabilized by the attractive electrostatic interaction dominated by the hydrogen in the N5 position i.e. only in case of ²[FADH⁺–O₂^{•-}] (H) and ³[FADH[•]–O₂^{•-}] (I) (see Figure 5). The HO₂[•] species resides always close to the FAD due to electrostatic interaction between the H of HO₂[•] and N5 of FAD (in case of ²[FAD_{ox}–HO₂] (J) and ³[FAD^{•-}–HO₂] (K)). On the contrary, triplet molecular oxygen diffuses out of the flavin pocket and that is independent of the redox and protonated states of the FAD. We observe only two distinct paths (shown with black arrows in Figure 4) via which the oxygen species moves outside of the lumiflavin pocket. After diffusing out from the flavin pocket, triplet oxygen is either stabilized or it hops between very few cryptochrome pockets except in the case of ⁴[FAD^{•-}–O₂] (B) where the triplet oxygen is hopping between several pockets.

Radical superoxide and hydroxyl radicals are essentially stabilized by electrostatic interactions and hydrogen bonding. To show this, we have computed the electrostatic potential due to the FAD species, Trp420 and Cys416 felt by the oxygen species for the final stable structure of ³[FADH[•]–O₂^{•-}] (I) and ³[FAD^{•-}–HO₂] (K) which are shown in Figure 5. The electrostatic potential (ESP) is calculated using Adaptive Poisson-Boltzmann Solver (APBS)³⁸ implemented in vmd³⁹. The ESP is shown in a RGB (Red-Green-Blue) color scale in a range of -0.05 to 0.05 k_bT/e . For system I, we can see that a positive potential (blue), with contribution from FAD, Trp420 and Cys416 group and dominated by the contribution from N5H group of lumiflavin, is created in the region around

the superoxide (shown in CPK representation) and therefore the superoxide, having negative electrostatic potential due to its' negative charge, is highly stabilized in that region due to strong electrostatic interaction. On the other hand, in system **K**, the negative ESP (red) around the $\text{FAD}^{\bullet-}$ stabilizes the HO_2^\bullet radical (shown in CPK representation in the lower panel of Figure 5) since HO_2^\bullet itself generate a positive electrostatic potential around the H atom. Finally, the triplet oxygen, having zero partial charge, does not feel any attractive potential and therefore can freely move in and around the binding pocket.

The hydrogen bonding between FAD and radical oxygen species stabilizes further ROS in the binding pocket. We observe that in fact hydrogen bonding induces a stronger binding of oxygen than the pure non-bonded electrostatic interactions. Indeed, the stabilization of hydroxyl radical strongly depends on the initial conditions, whereas this is not observed for the superoxide or triplet oxygen species. The HO_2^\bullet stays within the cavity only when the simulation is started from its favorable position (near N5 atom of FAD) which is true only if the $\text{O}_2^{\bullet-}$ takes proton from the N5H. This indicates that the hydrogen bonding between the N5H atom of radical or anionic FADH and OO2 atom of hydroxyl radical is the main electrostatic interaction between hydroxyl radical and FAD. If it forms HO_2^\bullet by taking proton from somewhere else of the protein or from solvent and is placed initially anywhere else than the favored position as shown in Figure 6, the HO_2^\bullet flies away from the C4a cavity. On the contrary, for the superoxide or triplet oxygen, the qualitative results that whether the oxygen species stays or leave the C4a cavity remain invariant on its initial position be it below the lumiflavin ring or in between the lumiflavin ring and adenine (in both case, close to the C4a atom). The binding location of the superoxide in the flavin pocket remain also the same. In order to investigate the possibility of formation of C4a-hydroperoxyflavin within the limit of molecular dynamics simulations, the distance between N5 of lumiflavin ring and OO2 of oxygen species is plotted in Figure 6, indicating the formation of a strong hydrogen bonding [N5-H...O₂] (with average donor-acceptor distance <3.0 Å) facilitating the formation of $\text{FAD}^{\bullet-} + \text{HO}_2^\bullet$ as described in Figure 2. The low fluctuation of the ROS due to this hydrogen bonding also indicates towards possibility of formation of C4a-hydroperoxyflavin as suggested by other kinetic experimental studies.^{18,20,26} In the previous studies, the origin of the H^+ to form HO_2^\bullet from $\text{O}_2^{\bullet-}$ was never discussed. From our MD simulation results, we propose that the N5 atom of FADH is most likely the proton donor to form the hydroperoxyl radical intermediate.

3.2 Formation of superoxide and hydroxyl radicals

Recent experiments have been able to detect superoxide and other ROS inside cryptochromes^{18–21}. In this section, we discuss on the possibility of formation of ROS from electronic structure theory, in order to determine the oxidation state of oxygen.

The generation of superoxide implies an electron transfer from radical/anionic flavin to triplet oxygen. From a molecular orbital picture, the transferred electron is initially located on a singly occupied molecular orbital (SOMO) of radical FAD, which is of π^*

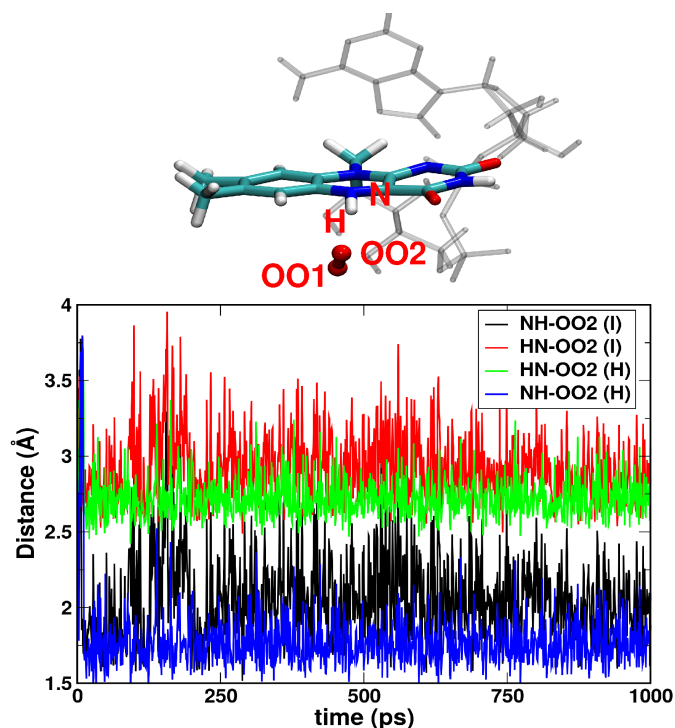


Fig. 6 HN5-OO2 and N5H-OO2 distances for a typical trajectory for $^2[\text{FADH}^+-\text{O}_2^-]$ (H) $^3[\text{FADH}^\bullet-\text{O}_2^\bullet]$ system (I) indicating strong tendency to form HO_2^\bullet radical. On top one typical structure (indicating the position of $\text{O}_2^{\bullet-}$ with respect to the N5 atom of FADH) out of thousands is shown.

character residing between the C4a-N5 atoms. This electron will be transferred to the highest occupied molecular orbital (HOMO) of $^3\text{O}_2$, which consists of π_x^* and π_y^* orbitals each containing one electron. These orbitals are degenerate when oxygen is in an isotropic environment but, inside the binding pocket of cryptochrome, the electron will be transferred to the π^* oxygen orbital that overlaps with the π^* orbital of FAD.

Upon photo-absorption, an electron is added to the triplet $[\text{FAD}_{\text{ox}}-\text{O}_2]$ complex leading either to a doublet or quartet total spin, depending on the relative orientation of the independent spins of oxygen and radical FAD, see Figure 7 where the contributing configuration state functions for a radical FAD- O_2 system with minimal active space CAS(3,3) are shown. In order to investigate the formation of superoxide, the energies of high and low spin states of different species involving radical oxygen are calculated using SA5-CASSCF+MS-CASPT2 method with larger active space of (11,12) for the radical semi-quinones and (12,12) for the reduced anion. These results are summarized in Table 1. It should be noted that, after validating that the main interaction with O_2 is localized in the lumiflavin ring, we considered only lumiflavin ring (instead of the full FAD cofactor) and oxygen in these calculations. The calculations are done on the structure of lumiflavin-oxygen species extracted from the highest populated dmCry- O_2 structure obtained using clustering analysis based on root mean square deviation implemented in Gromacs.

In Table 1, we report the three lowest energy states for

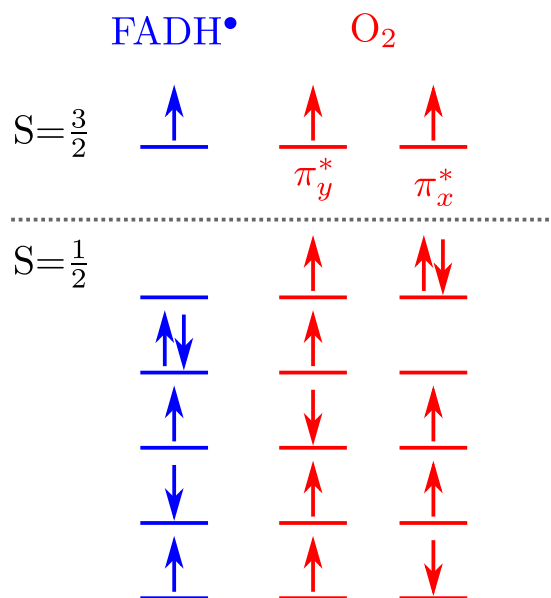


Fig. 7 Representation of the multiconfiguration wavefunction for a quartet ($S=3/2$) and doublet ($S=1/2$). The contributing configuration state functions for the $^4[\text{FADH-O}_2]^*$ ($S=3/2$) and $^2[\text{FADH-O}_2]^*$ ($S=1/2$) for the active space of CAS(3,3).

Table 1 SA5-CASSCF+MS-CASPT2 ground and excited state electronic energies for $[\text{FADH-O}_2]^*$, $[\text{FAD-HO}_2]^*$, $[\text{FADH-O}_2]^-$ and $[\text{FAD-HO}_2]^-$ species. For comparison, the ground state has been set to 0.00 as reference for each species independently. The states (St) are labeled by their spin (S for singlet, D for doublet, T for triplet and Q for quartet). Energies of first three states are shown for each spin. Spin multiplicity on oxygen species (Mult_{O_2}) is shown based on Mulliken spin density. All energies are in eV.

St	$[\text{FADH-O}_2]^*$		$[\text{FAD}_{\text{ox}}\text{-HO}_2]^*$	
	E_{ex}	Mult_{O_2}	E_{ex}	Mult_{O_2}
D0	0.09	2.32	0.00	2.00
D1	0.96	1.00	0.63	1.99
D2	0.98	1.00	2.30	–
Q0	0.00	2.94	2.27	2.00
Q1	1.70	2.96	2.74	1.99
Q2	3.35	2.03	3.28	2.00

St	$[\text{FADH-O}_2]^-$		$[\text{FAD}_{\text{ox}}\text{-HO}_2]^-$	
	E_{ex}	Mult_{O_2}	E_{ex}	Mult_{O_2}
S0	0.88	–	0.00	–
S1	0.97	–	0.53	–
S2	1.53	–	2.19	–
T0	0.00	2.91	0.04	2.00
T1	1.41	2.05	0.57	1.99
T2	1.65	1.98	2.23	2.00

each spin multiplicities of $[\text{FADH-O}_2]^*$ (doublet or quartet) and $[\text{FADH-O}_2]^-$ (singlet or triplet) species. In addition, we report the spin multiplicity of the oxygen fragment, extracted from the Mulliken analysis of the spin densities. First, we discuss the $[\text{FADH-O}_2]^*$ form. The lowest energy state corresponds to the quartet $^4[\text{FADH}^*\text{-O}_2]$, in which oxygen is in a triplet spin state. However, the lowest energy doublet state is energetically close (only 0.09 eV above Q0), suggesting that the doublet form can also exist ($^2[\text{FADH}^+\text{-O}_2^-]$). In that case, the oxygen spin state could not be precisely determined from the Mulliken analysis, but still its multiplicity is closer to a doublet oxygen form. After the proton transfer between FAD and superoxide, the $[\text{FAD}_{\text{ox}}\text{-HO}_2]^*$ complex is formed. The electronic structure calculations indicate that the doublet is the ground state, in which HO_2^\bullet has a doublet spin multiplicity. The lowest quartet state for this complex lays 2.26 eV above the doublet. Second, we discuss the $[\text{FADH-O}_2]^-$ complex. The results for this complex suggest that the ground state is a triplet $[\text{FADH-O}_2]^-$, in which oxygen is a triplet. The radical superoxide is only formed in the first excited triplet state (T1) which exists as $^3[\text{FADH}^*\text{-O}_2^-]$ and is ≈ 1.4 eV above the triplet ground state. On the other hand, in the lowest singlet state (which is 0.88 eV above the triplet ground state) doublet superoxide is also formed. Upon a proton transfer, the complex $\text{FAD}^{\bullet-}\text{-HO}_2^\bullet$ is formed. For this complex, both the lowest singlet and triplets are almost degenerate ($\Delta E = 0.038$ eV) and both of them contains doublet oxygen species $^2\text{HO}_2^\bullet$. The HO_2^\bullet is formed in doublet not only in the ground state, but also for all other excited states of singlet and triplet multiplicity.

3.3 The role of Trp420 and Cys416 in *Drosophila melanogaster* cryptochrome

Trp420 is the closest tryptophan to the FAD. It has been reported that the closest tryptophan or a tryptophan triad containing the closest tryptophan is the electron donor that reduces FAD upon photon absorption,⁸ thus forming $\text{TrpH}^{\bullet+}$ and subsequently Trp^\bullet . Therefore, Trp420 is likely to be in radical form while considering cryptochrome with reduced FAD. To investigate the effect of Trp^\bullet on the position of $\text{O}_2^{\bullet-}$, we ran further simulations for the $^2[\text{FADH}^+\text{-O}_2^-]$ (a typical system where superoxide binds to lumiflavin) with the Mulliken charges for Trp^\bullet and $\text{TrpH}^{\bullet+}$ calculated at the same level of theory as discussed in Section 2. Figure 8a shows the comparison of the position of cluster of superoxide with respect to the FADH^\bullet and tryptophan for neutral Trp420 (red) and $\text{TrpH}^{\bullet+}$ (blue) and Trp^\bullet (green). We observe that although the superoxide cluster is closer to the tryptophan for $\text{TrpH}^{\bullet+}$ (blue) than for the neutral Trp420 (red) due to strong attractive electrostatic interactions between the negative superoxide and positively charged NH^+ , it is closer to the FADH^\bullet or almost at the same position for Trp^\bullet (green) with respect to the system with Trp420 (red).

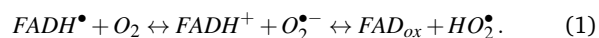
To illuminate on the probable proton donor in dmCry after the photoreduction of FAD, the crystal structure of plant cryptochrome and dmCry is superimposed and it is observed that Cys416 in dmCry is in the same position of Asp396 of plant cryptochrome (Figure 8b left panel). Since Asp396 is reported to be

the proton donor in plant cryptochrome⁸, by analogy, we propose Cys416 may act as a proton donor in dmCry. To further confirm this, an MD simulation run of 1 ns is performed for dmCry and the distance between the -SH of Cys416 and N5 of FAD is recorded and found them to be in close contact over the simulation time. Figure 3 shows the distance between the H of SH (Cys416) and N5 of the ISO(black)/N of the closest tryptophan, Trp420 (red) which indicates SH bond rotates freely- towards N5 of lumiflavin (to donate proton) and then towards NH of Trp420 (to get proton to compensate) which suggests that under favorable condition it is feasible that Cys416 can donate proton to semireduced anionic FAD and can get proton from tryptophan to compensate.

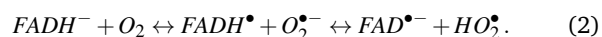
Cysteine has a pK_a value of 8.3 (in solution) which is close to physiological pH and therefore at the limit of acting as a proton donor. There have been studies in the literature on the possible role of cysteine as a proton donor in dmCry. Some spectroscopic studies suggested that the formation of FADH• in dmCry is hindered in physiological conditions, indicating that cysteine has a high pK_a value in protein.^{25,40} These would indicate that other residues in the cavity are responsible for the protonation of anionic radical semiquinonic flavin. At variance, Hong et al. used theoretical simulations to show that Cys416 pK_a is 9.7 in protein. They conclude that Cys416 could act as the proton donor, despite being less efficient than aspartic acid.⁴¹ Based on their pK_a calculations, the difference (2.1) between the pK_a of Asp396 in plant cryptochrome (7.6) and of Cys416 in dmCry (9.7) is smaller than the difference (4.4) of their pK_a in solution. Therefore, even though it is evident that FADH• is formed, it remains an open question whether Cys416 act as a possible proton donor or not. Cysteine can possibly act as a slow proton donor only at a higher pH value. A rigorous study based on constant pH molecular dynamics simulation would be necessary to confirm that.

3.4 FAD–O₂ as alternative radical pair for magnetoreception

Among the several reactions between FAD and oxygen species, there are four most important reactions involving a radical oxygen that is stabilized within the C4a cavity. Some of these reactions are also suggested to contribute to radical pair mechanism of magnetoreception by experimental spectral data¹⁸). The first two reactions correspond to the electron transfer from FADH• to O₂ followed by proton transfer from FADH⁺ to O₂^{•-}, that is,



The third and four reactions correspond to the electron transfer from FADH⁻ to O₂ followed by proton transfer from FADH• to O₂^{•-}, that is,



There exist thus two radical pairs which may act as “alternative” radical pair and they are FADH•+O₂^{•-} and FAD^{•-}+HO₂[•]. Still, there are few conditions to be satisfied for the radical pair mechanism for magnetoreception to work best: (i) the radical pair should be closely spaced for spin selective conversion, (ii) the electron nuclear hyperfine interaction should be weak, (iii)

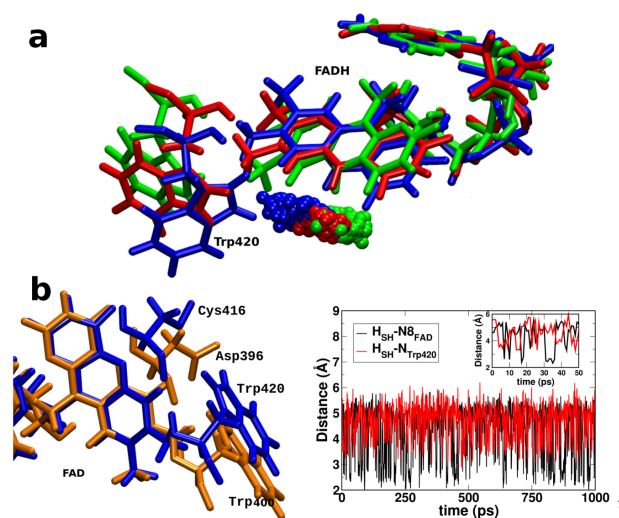


Fig. 8 (a) Comparison of the position of superoxide clusters for different redox and protonation states of tryptophan e.g. neutral Trp420 (red), Trp•H⁺ (blue) and Trp• (green). The structures are aligned with respect to the FADH•. (b) Left: comparison of the core active site (containing FAD, Trp400/Trp420 and Asp396/Cys416 of plant (orange) and *Drosophila melanogaster* (blue) cryptochrome. Right: the distance between Hydrogen of SH (Cys416) and N8 of lumiflavin ring of FAD (black)/N of Trp420 (red). The inset shows the first 50 ps (zoomed) to detect the frequency of the SH bond rotation.

the spin relaxation of the radical should be slow, and (iv) the exchange and dipole-dipole spin couplings should be close to zero or mutually cancelling.⁴² With the results we have reported, we can qualitatively say that these conditions are satisfied for both radical pairs involving oxygen. Indeed, from our MD simulations we showed that FADH•–O₂^{•-} and FAD^{•-}–HO₂[•] stays within 2–3 Å. The hyperfine coupling condition is more easily satisfied by oxygen species radical pair than by tryptophan radical pair, since its ¹⁶O and ¹⁸O isotopes are not magnetic. Therefore, the hyperfine coupling of the radical pair is only due to FADH•. For the spin relaxation, it is known that O₂^{•-} has a fast spin relaxation kinetics^{18,21}, but the presence of Trp• close to the radical pair (as shown in Figure 8) can act as scavenger to slow down the spin relaxation of oxygen species. In addition, the restricted mobility of radical pair (indicated by low fluctuation of oxygen species in Figure 3) due to strong electrostatic interactions can slow down the spin relaxation. Finally, from electronic structure calculations, we can estimate the exchange coupling strength as the difference between the low and the high spin lowest energies. From this criteria, we can conclude that only FAD^{•-}–HO₂[•] has a small exchange coupling ($J=400$ meV). From these results, we can conclude that FAD^{•-}–HO₂[•] is a good candidate for explaining magnetoreception via the “alternative” radical pair with oxygen.

4 Conclusion

In this work, we have systematically explored the fate of different oxygen species in the binding pocket of *Drosophila melanogaster* cryptochrome using atomistic molecular dynamics simulations, taking into account the charge and spin multiplicity of different FAD and oxygen forms that are generated upon blue light absorp-

tion. Additionally, we performed electronic structure simulations of different FAD–O₂ radical pairs to clarify the oxidation state of oxygen in each of the complexes.

The molecular dynamics simulations suggest that radical oxygen species are strongly stabilized close to FAD due to strong attractive electrostatic interactions and hydrogen bonding. On the contrary, triplet oxygen species move out of the cavity when FAD is in radical or charged form. The electrostatic attractive forces between the radical oxygen species and FADH is dominated by the interaction between N5H (of FADH[•]) and O₂^{•-}. The results also indicate to a strong tendency of formation of hydroperoxyl radical. The stability of hydroperoxyl radical near C4a atom are in agreement with previous studies suggesting formation of C4a-hydroperoxyflavin intermediate.²⁶

We show that the formation of hydroperoxyl radical is possible by the proton transfer from the proton at N5 position in FADH⁻. Furthermore, we have found that the varying electrostatic field of radical or neutral tryptophan has negligible impact on the position of oxygen. Still, the oxygen species are closer to the cationic TrpH^{•+} due to stronger electrostatic interactions. The four important systems that can lead to the formation of radical oxygen species are found to be ²[FADH⁺–O₂^{•-}], ²[FAD_{ox}–HO₂[•]], ³[FADH[•]–O₂^{•-}], ³[FAD^{•-}–HO₂[•]].

The electronic structure analysis suggests that the radical FADH–O₂ system in the ground state is a quartet and exist as ⁴[FADH[•]–O₂]. For this particular case, the ²[FADH⁺–O₂^{•-}] is only ≈0.1 eV above the ground state and therefore it is possible that both spin states are formed in the protein. For the [FADH–O₂]⁻ complex, the triplet radical pair ³[FADH[•]–O₂^{•-}] is 1.5 eV above the ground state ³[FADH⁻–O₂] in which oxygen is in a triplet. The only radical pair in the ground state is ³[FAD^{•-}–HO₂[•]] which has a small singlet-triplet energy gap.

In view of “alternative” radical pair, our MD results suggest that two probable radical pairs i.e. FADH[•]–O₂^{•-} and FAD^{•-}–HO₂[•]. Among them, FAD^{•-}–HO₂[•] passes all criteria as discussed in subsection 3.4. Although, more investigation is necessary on the lifetime of the short-lived hydroperoxyl radical. The FADH[•]–O₂^{•-} radical pair passes all criteria except the small exchange coupling criteria. Further investigation is needed on whether the cancellation of dipole and exchange coupling is possible⁴³. Environmental effects could also affect the order of states, but these are expected to be rather small in cryptochromes.⁴⁴

To summarize, our results from this study focuses not only on the qualitative position of different oxygen species in the flavoprotein active site, but also detect its binding location, diffusion pathway and surrounding important residues depending on varying electrostatic interactions. These results are important not only in view of investigating the “alternative” radical pair mechanism of magnetoreception but also shed light on several other functionality of flavoprotein in general e.g. ROS production, anti-oxidant defence. The results from our study (e.g. the specific binding location, diffusion pathway of oxygen species and surrounding residues with strong interactions) can help designing mutant flavoprotein to accelerate ROS production as well as to accelerate anti-oxidant defence mechanism.

Acknowledgments

The authors acknowledge financial support by the “Agence Nationale pour la Recherche” through the project BIOMAGNET (ANR-16CE29-0008-01). This work was granted access to the HPC resources of Aix-Marseille Université financed by the project Equip@Meso (ANR-10-EQPX-29-01) of the program «Investissements d’Avenir» supervised by the Agence Nationale de la Recherche.

References

- 1 V. Massey, *FASEB J.*, 1995, **9**, 473–475.
- 2 I. Chaves, R. Pokorny, M. Byrdin, N. Hoang, T. Ritz, K. Brettel, L. O. Essen, G. T. J. van der Horst, A. Batschauer and M. Ahmad, *Annu. Rev. Plant Bio.*, 2011, **62**, 335–364.
- 3 A. Sancar, *Chem. Rev.*, 2003, **103**, 2203–2237.
- 4 P. Sampathkumar, S. Turley, J. E. Ulmer, R. H. G., C. H. Sibley and W. G. Hol, *J. Mol. Biol.*, 2005, **352**, 1091–1104.
- 5 H. Myllykallio, G. Lipowski, D. Leduc, J. Filee, P. Forterre and U. Liebl, *Science*, 2002, **297**, 105–107.
- 6 E. Gross, K. D. B., C. A. Kaiser and D. Fass, *Cell*, 2004, **117**, 601–610.
- 7 K. R. Marshall, M. Gong, L. Wodke, J. H. Lamb, D. J. Jones, P. B. Farmer, N. S. Scrutton and A. W. Munro, *J. Biol. Chem.*, 2005, **280**, 30735–30740.
- 8 I. A. Solovy’ov, T. Domratcheva, A. R. Moughal Shahi and K. Schulten, *J. Am. Chem. Soc.*, 2012, **134**, 18046–18052.
- 9 C. T. Rodgers and P. Hore, *Proc. Nat. Acad. Sci.*, 2009, **106**, 353–360.
- 10 T. Ritz, S. Adem and K. Schulten, *BioPhys. J.*, 2000, **78**, 707–718.
- 11 Y.-T. Kao, C. Saxena, T.-F. He, L. Guo, L. Wang, A. sancar and D. Zhong, *J. Am. Chem. Soc.*, 2008, **130**, 13132–13139.
- 12 F. Cailliez, P. Müller, M. Gallois and A. de la Lande, *J. Am. Chem. Soc.*, 2014, **136**, 12974–12986.
- 13 R. J. Gegear, L. E. Foley, A. Casselman and S. M. Reppert, *Nature*, 2009, **463**, 804–807.
- 14 T. Ritz, R. Wiltschko, P. Hore, C. T. Rodgers, K. Stapput, P. Thalau, C. R. Timmel and W. Wiltschko, *Biophys. J.*, 2009, **96**, 3451–3457.
- 15 N. Christine, D. Susanne, S. Katrin, A. Margaret, P. Leo, W. Wolfgang and W. Roswitha, *J. Royal Soc. Interface*, 2013, **10**, 20130638.
- 16 D. R. Kattnig, *J. Phys. Chem. B*, 2017, **121**, 10215–10227.
- 17 D. R. Kattnig and P. J. Hore, *Sci. Rep.*, 2017, **7**, 11640–11650.
- 18 P. Müller and M. Ahmed, *J. Biol. Chem.*, 2011, **286**, 21033–21040.
- 19 L.-D. Arthaut, N. Jourdan, A. Mteyrek, M. Procopio, M. El-Esawi, A. d’Harlingue, P.-E. Bouchet, J. Witczak, T. Ritz, A. Klarsfeld, S. Birman, R. J. Usselman, U. Hoecker, C. F. Martino and M. Ahmad, *PLOS ONE*, 2017, **12**, 1–15.
- 20 L. van Wilderen, G. Silkstone, M. Mason, J. J. van Thor and M. T. Wilson, *FEBS open bio*, 2015, **5**, 885–892.
- 21 H. J. Hogben, O. Efimova, N. Wagner-Rundell, C. R. Timmel and P. J. Hore, *Chem. Phys. Lett.*, 2009, **480**, 118–122.

- 22 R. Baron, C. Riley, P. Chenprakhon, K. Thotsaporn, R. T. Winter, A. Alfieri, F. Forneris, W. J. H. van Berkel, P. Chaiyen, M. W. Fraaije, A. Mattevi and J. A. McCammon, *Proc. Nat. Acad. Sci.*, 2009, **106**, 10603–10608.
- 23 B. Giovani, M. Byrdin, M. Ahmad and K. Brettel, *Nat. Struct. Biol.*, 2003, **10**, 489–490.
- 24 R. Banerjee, E. Schleicher, S. Kacprzak, J. P. Bouly, M. Picot, W. Wu, A. Berndt, E. Wolf, R. Bittl and M. Ahmad, *J. Biol. Chem.*, 2007, **282**, 14916–14922.
- 25 A. Berndt, T. Kottke, H. Breitzkreuz, R. Dvorsky, S. Hennig, . Alexander, M and E. Wolf, *J. Biol. Chem.*, 2007, **282**, 13011–13021.
- 26 V. Massey, *J. Biol. Chem.*, 1994, **269**, 22459–22462.
- 27 J.-D. Chai and M. Head-Gordon, *Phys. Chem. Chem. Phys.*, 2008, **10**, 6615–6620.
- 28 M. M. Francl, W. J. Pietro, W. J. Hehre, J. S. Binkley, M. S. Gordon, D. J. DeFrees and J. A. Pople, *J. Chem. Phys.*, 1982, **77**, 3654–3665.
- 29 H. J. C. Berendsen, D. van der Spoel and R. van Drunen, *Comput. Phys. Commun.*, 1995, **91**, 43–56.
- 30 A. D. J. Mackerell, M. Feig and C. L. r. Brooks, *J. Comput. Chem.*, 2004, **25**, 1400–1415.
- 31 P. Bjelkmar, P. Larsson, M. A. Cuendet, B. Hess and E. Lindahl, *J. Chem. Theo. Comput.*, 2010, **6**, 459–466.
- 32 K. Vanommeslaeghe, E. Hatcher, C. Acharya, S. Kundu, S. Zhong, J. Shim, E. Darian, O. Guvench, P. Lopes, I. Vorobyov and A. D. MacKerell (Jr.), *J. Comp. Chem.*, 2010, **31**, 671–690.
- 33 M. J. Frisch, G. W. Trucks, H. B. Schlegel, G. E. Scuseria, M. A. Robb, J. R. Cheeseman, G. Scalmani, V. Barone, G. A. Petersson, H. Nakatsuji, X. Li, M. Caricato, A. V. Marenich, J. Bloino, B. G. Janesko, R. Gomperts, B. Mennucci, H. P. Hratchian, J. V. Ortiz, A. F. Izmaylov, J. L. Sonnenberg, D. Williams-Young, F. Ding, F. Lipparini, F. Egidi, J. Goings, B. Peng, A. Petrone, T. Henderson, D. Ranasinghe, V. G. Zakrzewski, J. Gao, N. Rega, G. Zheng, W. Liang, M. Hada, M. Ehara, K. Toyota, R. Fukuda, J. Hasegawa, M. Ishida, T. Nakajima, Y. Honda, O. Kitao, H. Nakai, T. Vreven, K. Throssell, J. A. Montgomery, Jr., J. E. Peralta, F. Ogliaro, M. J. Bearpark, J. J. Heyd, E. N. Brothers, K. N. Kudin, V. N. Staroverov, T. A. Keith, R. Kobayashi, J. Normand, K. Raghavachari, A. P. Rendell, J. C. Burant, S. S. Iyengar, J. Tomasi, M. Cossi, J. M. Millam, M. Klene, C. Adamo, R. Cammi, J. W. Ochterski, R. L. Martin, K. Morokuma, O. Farkas, J. B. Foresman and D. J. Fox, *Gaussian 16 Revision A.01*, 2016, Gaussian Inc. Wallingford CT.
- 34 A. D. MacKerell (Jr.), D. Bashford, M. Bellott, R. L. R. L. Dunbrack (Jr.), J. D. Evanseck, M. J. Field, M. Fischer, J. Gao, H. Guo, S. Ha, D. Joseph-McCarthy, L. Kuchnir, K. Kuczera, F. T. K. Lau, C. Mattos, S. Michnick, T. Ngo, D. T. Nguyen, B. Prodhom, W. E. Reiher, B. Roux, M. Schlenkrich, J. C. Smith, R. R. Stote, J. Straub, M. Watanabe, J. WiÅrkiewicz-Kuczera, D. Yin and M. Karplus, *J. Phys. Chem. B*, 1998, **102**, 3586–3616.
- 35 F. Autenreith, J. Tajkhorshid, E. and Baudry and Z. Luthey-Schulten, *J. Comp. Chem.*, 2004, **25**, 1613–1622.
- 36 B. O. Roos, V. Veryazov and P.-O. Widmark, *Theor. Chem. Acc.*, 2004, **111**, 345–351.
- 37 F. Aquilante, J. Autschbach, R. K. Carlson, L. F. Chibotaru, M. G. Delcey, L. De Vico, I. Fdez. GalvÃn, N. FerrÃl, L. M. Frutos, L. Gagliardi, M. Garavelli, A. Giussani, C. E. Hoyer, G. Li Manni, H. Lischka, D. Ma, P. Ã. Malmqvist, T. MÃjller, A. Nenov, M. Olivucci, T. B. Pedersen, D. Peng, F. Plasser, B. B. Pritchard, M. Reiher, I. Rivalta, I. Schapiro, J. Segarra-MartÃ, M. Stenrup, D. G. Truhlar, L. Ungur, A. Valentini, S. Vancoillie, V. Veryazov, V. P. Vysotskiy, O. Weingart, F. Zapata and R. Lindh, *J. Comput. Chem.*, 2016, **37**, 506.
- 38 N. Baker, D. Sept, S. Joseph, M. J. Holst and M. J. A., *Proc. Nat. Acad. Sci.*, 2001, **98**, 10037–10041.
- 39 W. Humphrey, A. Dalke and K. Schulten, *J. Molec. Graphics*, 1996, **14**, 33–38.
- 40 B. Paulus, C. Bajzath, F. Melin, L. Heidinger, V. Kromm, C. Herkersdorf, U. Benz, L. Mann, P. Stehle, P. Hellwig, S. Weber and E. Schleicher, *FEBS Journal*, 2015, **282**, 3175–3189.
- 41 G. Hong and R. Pachter, *J. Phys. Chem. B*, 2015, **119**, 3883–3892.
- 42 P. J. Hore, *Annu. Rev. BioPhys.*, 2016, **45**, 299–344.
- 43 O. Efimova and P. J. Hore, *BioPhys. J.*, 2008, **94**, 1565–1574.
- 44 E. Cannuccia, O. Pulci, R. D. Sole and M. Cascella, *Chem. Phys.*, 2011, **389**, 35 – 38.